Available online at www.scholarsresearchlibrary.com

Scholars Research Library

Archives of Physics Research, 2010, 1 (4): 126-136
(http://scholarsresearchlibrary.com/archive.html)

Scholars Research Library
ISSN 0976-0970
CODEN (USA): APRRC7

Pitch Angle Loss-Cone Anisotropic Magneto plasma in Presence of Parallel Electric A.C. Field

[#1]R S Pandey, [#1]U C Srivastava, [#2]A K Srivastava, [#3]S Kumar and [#3]D K Singh

[#1]Department of Physics Amity Institute of Applied Sciences, Amity University, Noida, UP,
[#2]Department of Physics Jagatpur P.G. College Jagatpur Varanasi, UP,India
[#3]Department of Physics Nalanda College Biharsharif Nalanda MU Bodh Gaya Bihar, India

---

ABSTRACT

In present paper electromagnetic wave has been studied in the presence of parallel A.C. electric field for pitch angle loss-cone anisotropic magneto-Plasma. The detail derivation of dispersion relation and growth rate has been done by using the method of characteristics solution and kinetic approach. The effect A.C field frequency and magnetite of A.C. field has been studied and discussed in the result section. The pitch angle anisotropy is the prime source of instability.

Keywords: Anisotropic magneto-Plasma, Magnetosphere, Growth/decay of wave, pitch angle.

INTRODUCTION

Ducted whistlers have been used to study plasma properties in the equatorial region of the magnetosphere and the mapping of the spatial distribution and the drift of plasma within the plasma sphere in the range of 2-6 earth radii. Earlier works in this regard involved the recording of naturally occurring whistler waves at ground stations to explore the existence, dynamic, and levels of large scale density irregularities, magnetic and electric field properties, plasma particle distribution and the growth / decay of these waves [1, 2, 3]. Recently however, artificially triggered/ stimulated emissions (ATE's or ASE's) have been produced by Signal transmitted from ground stations and VLF wave injection experiments, like the one of ISEE-A spacecraft, Explorer 45 and Imp– 6[4,5,6,7] and have been used to study the magnetosphere as well as for both controlling and sensing its properties. These VLF whistler mode waves excited by the injection of artificial free energy source into the magnetosphere from ground of from rockets/ Satellites have been observed to produce a variety of interesting and important effects, with the injection of the triggering signal having the additional advantage of being controllable contrary to the natural sources. Theory and computer simulations of magnetospheric VLF emissions by signals of sufficient strength and duration have also been a subject of a more recent study [8]. Space time evolution of whistler mode wave growth in the magnetosphere triggered by injection

of signal frequency 2-6 KHz wave pulse have also been studied by computer simulation techniques [9,10].

A number of theories have also been put forth to explain the phenomena of triggered emission of whistlers in the magnetosphere [11] and presently there is a general agreement that the emission triggering process involves a mechanism that could be called a cyclotron –wave-particle interaction or wave-wave interaction, the inhomogeneity in density and magnetic field [12,13]. Wave-particle interaction consist of non linear interaction between a finite amplitude wave train and the particles that happen to be in resonance with it, i.e., those particles which see the electric and magnetic field vectors of the wave rotates at the local gyrofrequency (those which moves at approximately the resonant velocity) and are able to exchange energy with the wave over an extended period of time. Cyclotron resonance as a mechanism for whistler wave growth, first suggested by Dungey [14], has been the basis for most of the theoretical treatment and simulations which followed. Such interactions between the wave and the particles resonating with it (cyclotron-wave-particle interactions) result in the distortion of the particle velocity distribution function near the resonance velocity which in turn lead to either collision less amplification or damping of the wave depending on the distribution of the electrons.

In all theoretical studies, the geomagnetic field B_0, the number density n_0 of the low energy electrons, and the density and velocity distribution of resonant energy electron are the physical properties of the magnetosphere relevant to the ATE generation. The accuracy of any theoretical treatment of the whistler technique to study the magnetosphere and the plasma properties therein, therefore, depend on the use of accurate magnetic field and plasma models of the magnetosphere. The traditional dipole magnetic field model and a model of plasma distribution along field lines based on constant–temperature diffusion equilibrium do not obviously suffice.Furthermore, increased use of the whistler technique in conjunctions with ATE's and in situ wave injection methods to study the magnetosphere and observation of phenomena at lower latitudes has necessitated the use of more realistic magnetospheric and plasma parameter models available.

In the frame of laboratory studies devoted to whistler excitation by a modulated electron beam injected in a magneto plasma under conditions relevant to space experiments, fast processes have been investigated by Starodubtsev and Kraft [15] using the modulated electron beam as a train of short time current pulses injected in the after glow plasma with an energy of the order of 300 eV. Plasma responses to the fast perturbations are transported by whistler waves. Different types of responses have been evidenced and characteriezed depending on the nature of the whistler excitation mechanism involved. Non-resonant transition radiation from the beam injection point and Cherenkov resonant transition radiation from the beam injection point and Cherenkov resonant emission. Both emissions could be distinguished one from each other owing to adequate choices of plasma parameters and observation conditions. The formation of wake field associated with the propagating current pulses has also been observed for first time tin the whistler range. This study should shed light on the physical mechanisms connected with the injection of modulated and pulsed electron beams in space plasmas, as well as on fast processes induced in the whistler frequency range by the presence of superthermal fluxes of electrons traveling in the ionospheric and magnetospheric plasma. Misra and Haile [16] has been studied parallel propagating electromagnetic whistler mode instability in the presence of parallel A.C. electric field for bi-Maxwellian distribution function and reported the effect of a.c.frequency and magnitude of a.c.electric field. Huang et al [17] calculated the characteristics of the incoherent whistler mode waves generated in the magnetosphere along the L= 5 geomagnetic field line which intersect the atmosphere in the region where the pulsating aurora is frequently observed and considered their implications for the pulsating aurora. They observed for the loss-cone

driven Whistler instability, the growth rate along the L = 5 field line in largest just above the ionosphere where the loss-cone angle is also large.

Due to motivation from above studies the present paper parallel propagation electromagnetic wave has been studied with parallel A.C. electric field for pitch angle loss-cone anisotropy magneto plasma. The detail derivation of dispersion relation and growth rate has been calculated by using the method of characteristics solution. The effect of pitch angle anisotropy and A.C. field frequency and magnitude of A.C. field has been discussed.

Dispersion relation and Growth rate

The plasma under consideration is of infinite extent embeded with a uniform magnetic field $\mathbf{B_0}$ ($\mathbf{B_0}\ \hat{e}_z$) and an electric field $E_0 \sin \nu t\ \hat{e}_z$, and whose distribution function $f(r,\mathbf{v},t)$ is governed by the Boltzmann equation. In the collision less case the self – consistent Vlasov – Maxwell equations to be used are

$$\frac{\partial f_s}{\partial t} + v.\frac{\partial f_s}{\partial r} + \frac{e_s}{m_s}\left[E + \frac{v \times B}{c}\right]\frac{\partial f_s}{\partial v} = 0 \qquad . (1)$$

and

$$\nabla.E = \sum_s 4\pi e_s \int d^3 v f_s$$

$$\nabla \times B = \sum_s \frac{4\pi e_s}{e} \int d^3 v.\ v f_s + \frac{1}{c}\frac{\partial E}{\partial t} \qquad (2)$$

$$\nabla.B = 0$$

$$\nabla \times E = -\frac{1}{c}\frac{\partial B}{\partial t}$$

Here the subscript *s* denotes the particle species, *i.e.,* for ions and electrons respectively. The electric field E_0 and the magnetic field B_0 represent the resultants of the external A.C field and magnetic field together with the self – consistent characteristic oscillations of E and B. & all other symbols have their usual meanings.

In this analysis A.C frequency has been assumed much smaller than the plasma and gyro frequency and the collision frequency negligibly small and independent of particle velocity, where as the thermal velocity of the background electrons are much larger than induced velocity due to AC field. In order to find the dispersion relation, first the motion of the particles (trajectories) in the given fields are computed and the perturbed distribution function, which depends on the integrals of motion, is then determined following a method similar to that adopted by Harris [19]. In case, the Vlasov-Maxwell equations (1) are liberalized. The linear zed equations obtained after neglecting the higher order terms and separating the equilibrium and non- equilibrium parts, following the techniques of Pandey et al [20] are given as

$$v\frac{\partial f_{s0}}{\partial r}. + \frac{e_s}{m_s}\left[E_o \sin \upsilon t + (v \times B_o)\right]\left(\frac{\partial f_{so}}{\partial v}\right) = 0 \qquad (3)$$

$$\frac{\partial f_{s1}}{\partial t} + v.\frac{\partial f_{s1}}{\partial r} + \left(\frac{F}{m_s}\right)\left(\frac{\partial f_{s1}}{\partial v}\right) = S(r,v,t) \qquad (4)$$

where force is defined as $F = m\,dv/dt$

$F = e_s[E_{0z}\sin\upsilon t + (v\times B_0)]$ (5) Following methods and techniques of Misra & Pandey[18]; Pandey et al [20] the unperturbed particle trajectories are obtained by using the equation of motion(5) and *S(r,v,t)* is defined as

$$S(r,v,t,) = -\left(\frac{e_s}{m_e}\right)\left[E_1 + \frac{(v\times B_0)}{c}\right].\left(\frac{\partial f_{so}}{\partial v}\right) \qquad (6)$$

The method of characteristics solution is used to determine the perturbed distribution function which is obtained from equation (4) by

$$f_1(r,v,t) = \int_0^\infty S\{r_0(r,v,t,), v_0(r,v,t)), t-t'\}dt \qquad (7)$$

We have transformed the phase space co-ordinate system from (r, v, t) to (r_0, v_0 ,t - t') and t'=t - t'. The particle trajectories that have been obtained by solving equation (5) for given external field configuration.

$$x_0 = x + \frac{v_y}{\omega_{cs}} - \frac{1}{\omega_{cs}}(v_x\sin\omega_{cs}t' + v_y\cos\omega_{cs}t')$$

$$y_0 = y + \frac{v_x}{\omega_{cs}} - \frac{1}{\omega_{cs}}(v_x\cos\omega_{cs}t' + v_y\sin\omega_{cs}t')$$

$$z_0 = z - v_z t' + \frac{\Gamma_z}{\upsilon^2}\sin\upsilon t' - \frac{\Gamma_z}{\upsilon}t \qquad (8)$$

and the velocities as

$$v_{xo} = v_x\cos\omega_{cs}t' - v_y\sin\omega_{cs}t'$$

$$v_{yo} = v_x\sin\omega_{cs}t' - v_y\cos\omega_{cs}t'$$

$$v_{zo} = v_z + \frac{\Gamma_z}{\upsilon}(\cos\upsilon t' - 1) \qquad (9)$$

Where $\omega_{cs} = e_sB_0/m_s$ is the cyclotron frequency and $\Gamma_z = e_sE_{0z}/m_s$, υ = A.C.electric field frequency.

Equation (6) can be written in terms of perturbed quantities as

$$S(r_0, v_0, t-t') = \frac{e_s}{m_s\omega}e^{i(k.r(r,v,t') - \omega(t-t')}\times\left[(\omega - k.v_0)E_1 + (v_0.E_1)k\right]\frac{\partial f_0}{\partial v} \qquad (10)$$

After substituting from eq,(8) and (9) and doing some lengthy algebraic simplifications. One obtains by figure1 of Misra and Haile [16] with ac electric field in the z direction. Now using equation Eq. (6) and carrying out the time integration gives the first order perturbed distribution function $f_1(r,\mathbf{v},t)$ as

$$f_1(r,v,t) = \frac{-ie}{m\omega}\sum_{m,n,p}\frac{J_m(\lambda_1)J_p(\lambda_2)e^{i(m-n)\alpha}}{\left(\omega - k_\parallel v_\parallel - \frac{k_\parallel\Gamma_z}{\upsilon} - n\omega_c + p\upsilon\right)}$$

$$\left[U^{*}E_{1x}\frac{n}{\lambda_1}J_n(\lambda_1) - iU^{*}E_{1y}J'_n(\lambda_1) + W^{*}E_{1z}J_n(\lambda_1)\right] \qquad (11)$$

where Bessel identity has been used

$$e^{i\lambda\sin\alpha} = \sum_{k=-\infty}^{\infty} j_k(\lambda)e^{ik\alpha}$$

Where

$$U^{*} = \frac{1}{v_\perp}\frac{\partial f_0}{\partial v_\perp}\left[(\omega - k_\parallel v_\parallel)v_\perp + \frac{k_\parallel \Gamma_z}{\upsilon}v_\parallel\left(1-\frac{p}{\lambda_2}\right)\right]\left(\frac{\partial f_0}{\partial v_\parallel}\right)k_\parallel v_\perp$$

$$W^{*} = \frac{1}{v_\perp}\frac{\partial f_0}{\partial v_\perp}\left[v_\parallel n\omega_c - \frac{\Gamma_z}{\upsilon}n\omega_c\left(1-\frac{p}{\lambda_2}\right)\right]$$

$$\lambda_1 = \frac{k_\perp v_\perp}{\frac{\omega}{c}},\ \lambda_2 = \frac{k_\parallel \Gamma_z}{\upsilon^2} \text{ and } J'_n(\lambda_1) = \frac{dJ_n(\lambda_1)}{d\lambda_1} \qquad ...(12)$$

Where Bessel function arguments $\lambda_1,\ \lambda_2$ are defined in equation (12). Following Misra and Haile [16] and Misra and Pandey [21] the conductivity tensor $\|\sigma(k,\omega)\|$ is written as

$$\|\sigma(k,\omega)\| = -i\sum_{n.p}\frac{e^2}{m\omega}\int J_p(\lambda_2)\frac{S_{ij}d^3v}{\omega - k_\parallel v_\parallel - \frac{k_\parallel\Gamma_z}{\upsilon} + p\upsilon - n\omega_c} \qquad (13)$$

where

$$S_{ij} = \begin{vmatrix} v_\perp U^{*}\left(\frac{n}{\lambda_1}J_n\right)^2 & iv_\perp U^{*}\frac{n}{\lambda_1}J_nJ'_n & v_\perp W^{*}\frac{n}{\lambda_1}J_n^2 \\ iv_\perp U^{*}\frac{n}{\lambda_1}J_nJ'_n & v_\perp U^{*}J'^2_n & iv_\perp W^{*}J_nJ'_n \\ v_\parallel U^{*}\frac{n}{\lambda_1}J_n^2 & -iv_\parallel U^{*}J_nJ'_n & v_\parallel W^{*}J_n^2 \end{vmatrix} \qquad (14)$$

Now from $j = \|\sigma(k,\omega)\|E_1$ and Maxwell's curl equations for the perturbed quantities, one can get the dielectric tensor as

$$\left\|\varepsilon_{ij}(k,\omega)\right\| = 1 + \sum_{n.p}\frac{4\pi e^2}{m\omega^2}\int J_p(\lambda_2)\frac{S_{ij}d^3v}{\left(\omega - k_\parallel v_\parallel - \frac{k_\parallel\Gamma_z}{\upsilon} + p\upsilon - n\omega_c\right)} \qquad (15)$$

For whistler mode instabilities the general dispersion relation reduces to

$$\varepsilon_{11} \pm \varepsilon_{12} = N^2 \qquad (16)$$

Unperturbed velocity distribution function can be written from Huang et al [18] as

$$f_0 = \frac{n_0}{\pi^{3/2}\alpha_\perp^2\alpha_\parallel M}\exp\left[-\left(\frac{v_\perp}{\alpha_\perp}\right)^2 - \left(\frac{v_\parallel}{\alpha_\parallel}\right)^2\right] \quad (17)$$

Where the parallel and perpendicular thermal velocities are

$$\alpha_\perp = \left(\frac{K_B T_\perp}{m}\right)^{1/2}, \quad \alpha_\parallel = \left(\frac{K_B T_\parallel}{m}\right)^{1/2}, \quad A_T = \frac{\alpha_\perp^2}{\alpha_\parallel^2} - 1$$

$$M = \frac{1}{\sqrt{\frac{1+\tan^2\theta}{A_T+1}}}, \quad d^3v = 2\pi\int_0^\infty v_\perp dv_\perp \int_{-\infty}^\infty dv_\parallel \quad (18)$$

Where θ is loss-cone angle. After using eqs (14),(15),(16),((17),(18) and doing velocity integration and applying condition $k^2c^2/\omega 2 >>1$ the dispersion relation of whistler wave is obtained for $n=1, p=1$ and $J_p=1, J_q=1$

$$\frac{k^2c^2}{\omega_p^2} = \sum J_p(\lambda_2)\left[\left(\frac{\omega}{Mk_\parallel\alpha_\parallel} + X_z\right)Z(\xi(+A_T(1+\xi Z(\xi)) + \tan^2\theta\left\{\left(\frac{1}{2}\right) + \xi^2(1+\xi Z(\xi))\right\}\right] \quad (19)$$

where

$$X_z = p\upsilon - \frac{k_\parallel \Gamma_z}{\upsilon}, \quad \xi = \frac{\omega - \omega_c + p\upsilon - \frac{k_\parallel\Gamma_z}{\upsilon}}{Mk_\parallel\alpha_\parallel}, \quad \omega_p^2 = \frac{4\pi e_s^2 n_0}{m} \text{ (Plasma frequency)}$$

The required expression for growth rate and real frequency are obtained by using the standard definition as

$$\frac{\gamma}{\omega_c} = \frac{\frac{\sqrt{\pi}}{M\bar{k}}\left[\left(A_T - \frac{k_4}{k_3} + \frac{\tan^2\theta\ k_3^2}{M\bar{k}}\right)\right]k_3^3\exp\left(-\left(\frac{k_3}{M\bar{k}}\right)^2\right)}{\left\{1 + \frac{M^2\bar{k}^2}{2k_3^2} - \frac{M^2\bar{k}^2}{k_3}\left(A_T - \frac{k_4}{k_3}\right)\right\}} \quad (16)$$

$$X_3 = \frac{M^2\bar{k}^2}{\beta}\left[\frac{1}{2M^2} + \frac{A_T\beta}{2(1-X_4)^2}\right](1-X_4) \quad (17)$$

where

$$\beta = \frac{k_\beta k_\parallel n_0\mu_0}{B_0^2}, \quad \bar{k} = \frac{k_\parallel\alpha_\parallel}{\omega_c}, \quad k_3 = 1 - X_3 - X_4$$

$$k_4 = X_3 + X_4, \quad X_4 = \frac{p\upsilon - \frac{k_\parallel\Gamma_z}{\upsilon}}{\omega_c}$$

Plasma Parameters

Numerical evaluation of growth/ damping rate for whistler waves in the presence of AC electric field has been carried out for following[16,17] magnetospheric conditions, B_0= 1 x 10^{-7}T, n_0 = 5 x $10^6 m^{-3}$ L = 7. The range of anisotropy variation has been taken from 0.25 to0.75, AC field frequency from 2kHz to 8kHz, magnitude of AC electric field E_0 from zero to 20mV/m. The thermal energy of electrons is supposed to vary from 5 keV to 10keV and pitch angle anisotropy from 0 to 20 degree.

RESULTS AND DISCUSSION

In Fig (1) shows variation of growth rate γ/ω_c and real frequency $\omega_r/\ \omega_c$ with $\bar{k}$ for different values of the A C electric field frequencies at other given plasma parameters. It is clear from the figure that as the frequency of the AC field increases, the growth rate goes on decreasing with the decreases of the band width, at the same time the maxima shifts towards the lower $\bar{k}$ values. The Increase of A C frequency has no effect on the value of the real frequency. Fig (2) Shows variation of growth rate γ/ω_c and real frequency $\omega_r/\ \omega_c$ with $\bar{k}$ for different values of the magnitude of AC electric field E_0 at other given plasma parameters. The magnitude of AC electric field does not affect the value of real frequency. The growth rate along with the band width slightly increases with the increase of the magnitude of AC field. This is clear when compared with the increase of the magnitude of AC field. This is clear when compared with the growth rate curve in the absence of A C field. Although the effect of the magnitude of the AC field (E_0) on the growth rate is seen to be small, this is in conformity with the observations [17] that a minimum magnitude of signal is required to trigger the emissions and further increase in the magnitude is insignificant.

Fig (3) Shows variation of growth rate γ/ω_c and real frequency $\omega_r/\ \omega_c$ with $\bar{k}$ for different values of the temperature anisotropy, other plasma parameters being same as given in the plasma parameter section. There is no effect of anisotropy variation on the real frequency but the increase of temperature anisotropy increases the value of growth rate, decreasing the band width, and shifting the maxima towards lower $\bar{k}$ values. These observations imply that the thermal anisotropy is the major source of free energy for the instability.

Fig (4) Shows variation of growth rate γ/ω_c and real frequency $\omega_r/\ \omega_c$ with $\bar{k}$ for different values of the temperature $k_B T_{\|}$. The change in the energy of the electrons does not have any effect on the value of the real frequency. But the increase of energy ($k_B T_{\|}$) increases the growth rate and the band width as well. The increase in energy also shifts the maxima of the growth rate towards higher values of $\bar{k}$. This shows that the thermal energy of the electrons is the additional source of free energy for the instability. In Fig (5) the growth rate and real frequency is plotted against $\bar{k}$ for various values of the loss-cone angle in the presence of temperature anisotropy for other fixed plasma parameters. It shows that with the increase of the loss-cone angle, the growth rate goes on increasing simultaneously increasing the bandwidth. This indicates that the loss cone angle is supposed to provide additional energy for generating Whistler wave of low frequencies.

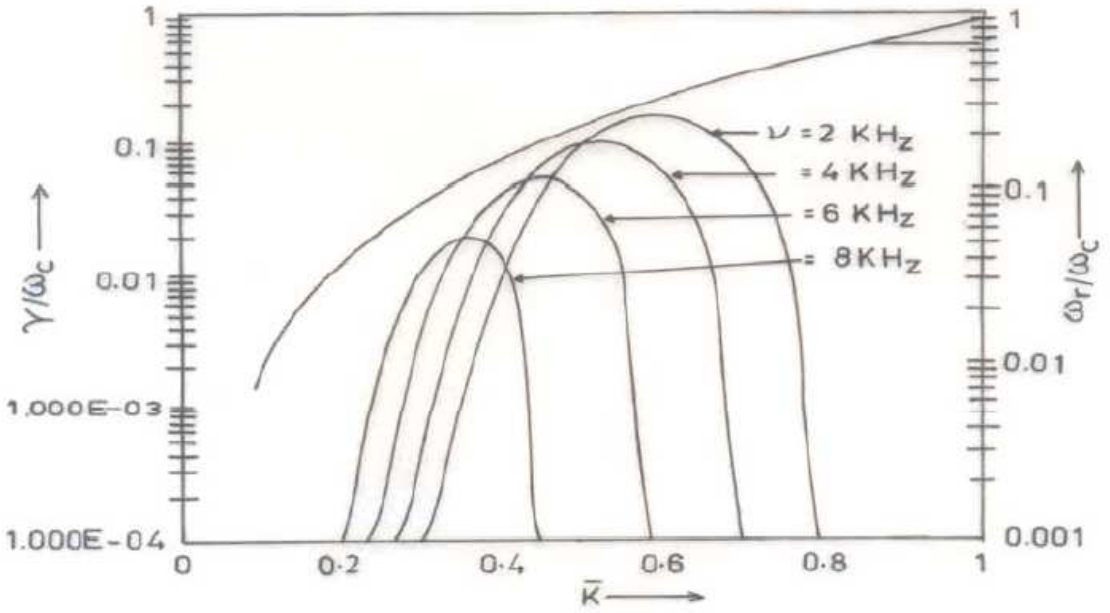

Fig.1 Variation of growth rate γ/ω_c and real frequency ω_r/ω_c with $\bar{k}$ for various Values of a.c.frequency and others parameters are fixed.

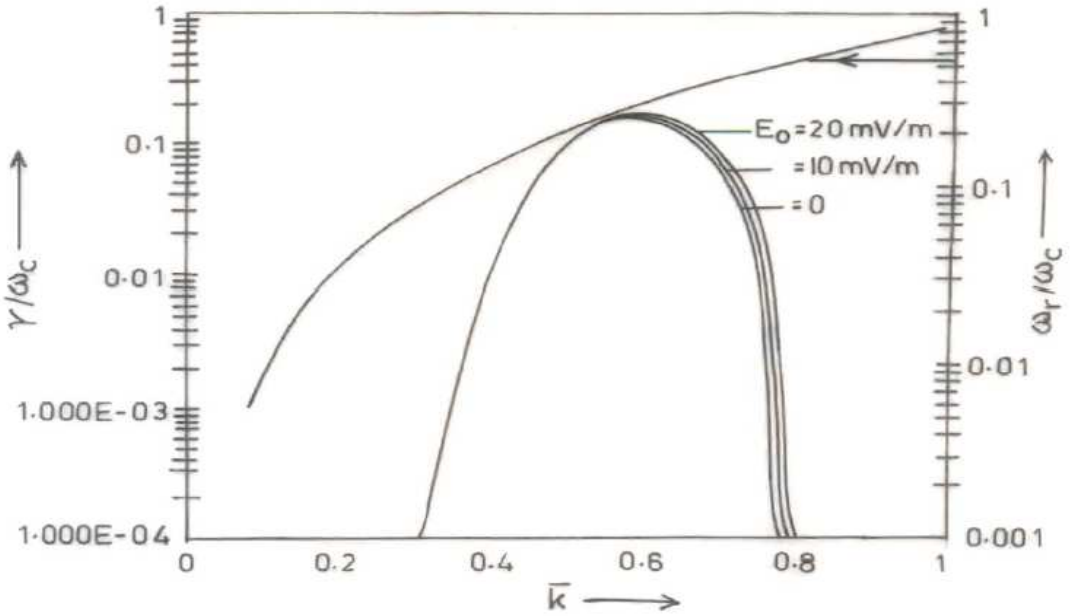

Fig.2 Variation of growth rate γ/ω_c and real frequency ω_r/ω_c with $\bar{k}$ for various Values of magnitude of a.c.electric field and others parameters are fixed.

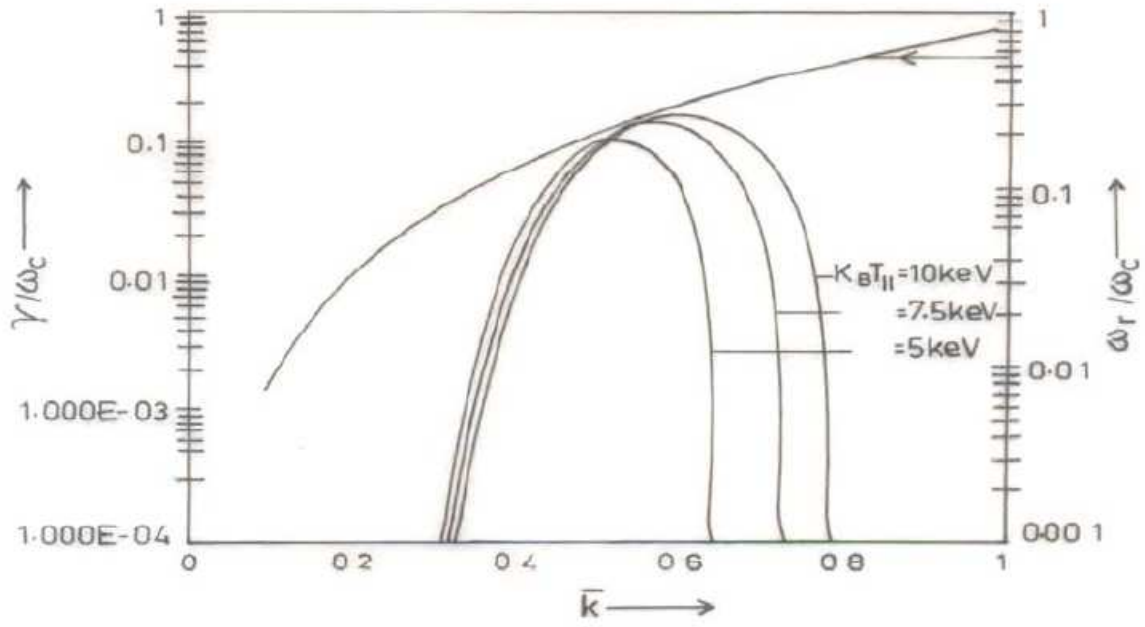

Fig.3 Variation of growth rate γ/ω_c and real frequency ω_r/ω_c with $\bar{k}$ for various Values of thermal velocity and others parameters are fixed.

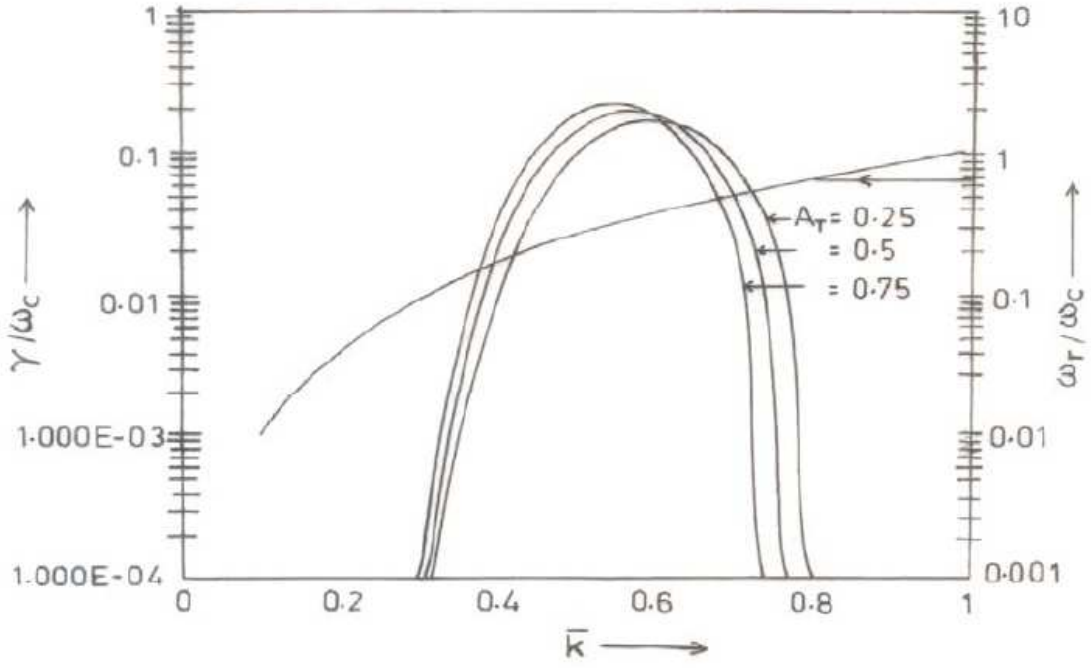

Fig.4 Variation of growth rate γ/ω_c and real frequency ω_r/ω_c with $\bar{k}$ for various Values of temperature anisotropy and others parameters are fixed.

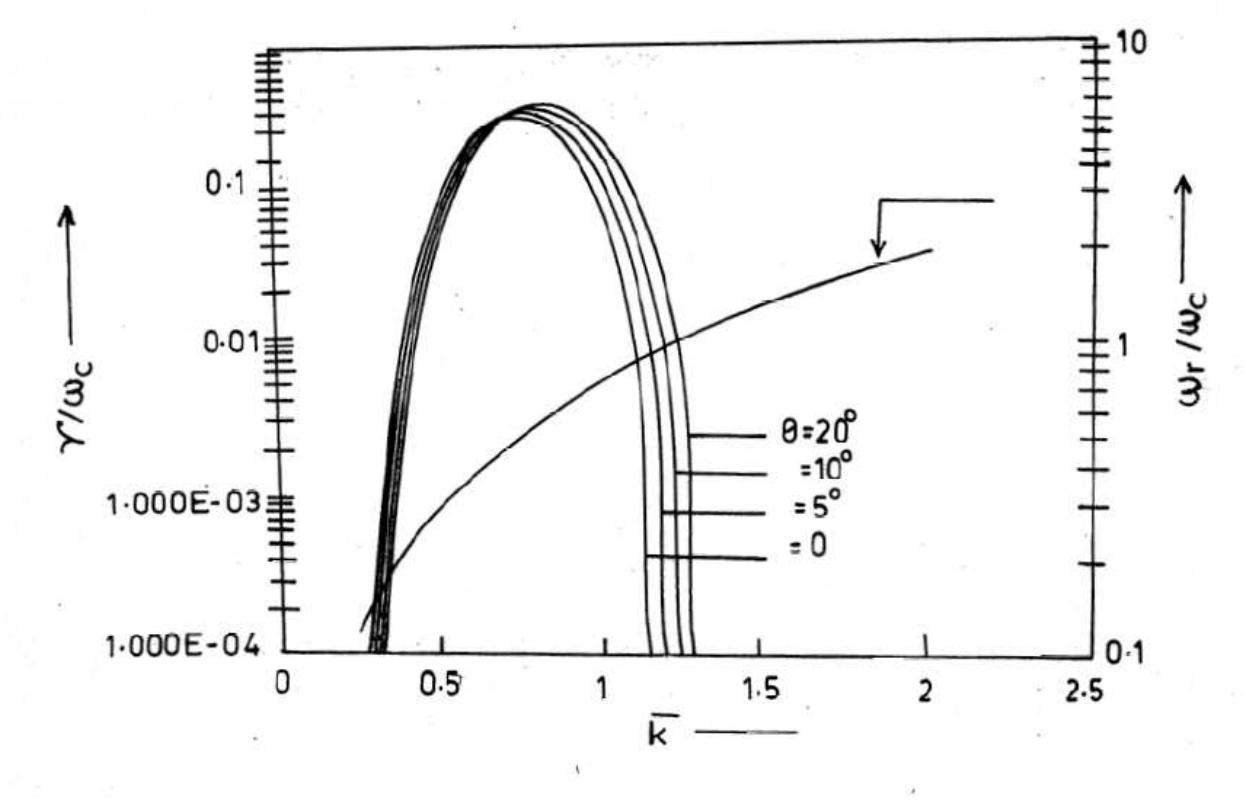

Fig.5 Variation of growth rate γ/ω_c and real frequency ω_r/ω_c with $\bar{k}$ for various Values of pitch angle anisotropy and others parameters are fixed.

CONCLUSION

The effect of a.c. frequency on the growth rate has been discussed in the result and discussion section. The growth rates and nature of curves are compared with well known results of Misra and Halie[16] and Pandey and Misra [21].The nature of curves are similar but the order of growth rate is different due to pitch angle anisotropy. The growth rate decreases by increasing the value of a.c. frequency is due to modification in resonant frequency. It means due to change in Doppler shifting frequency. The effect of pitch angle anisotropy from figure 5 deals that only temperature anisotropy is not a prim source of instability but pitch angle anisotropy is also a free energy source of instability. In the absence of temperature anisotropy growth rate also increases by increasing the pitch angle anisotropy.

REFERENCES

[1] Helliwell, R.A.," Whistlers and related ionospheric phenomena", Stanford Univ. Press, Stand ford, Calif, (**1965**).
[2] Thomson, R.J. and Dowden, R.L, *J. Atmos, Terr Phys.* a 39, 869, (**1977**).
[3] Sazhin, S.S, Hayankawa, M. and Bullough, K., *Ann.Geophys*. 10, 293, (**1992**).
[4] Helliwell, R.A.and Katsuprakis, J.P, *J. Geophys. Res*., 79, 2511, (**1974**).
[5] Inan U.S., Bell, T.F., Carpender, D.L. and Anderson, R.R., *J. Geophys. Res*., 82, 1177, (**1977**)a.
[6] Bell, T.F. and Helliwell R.A.," The Stanford University VLF wave injection experiment on the ISEE-A spacecraft "IEEE Trans. Geosc. Elect. GE-16, 248, (**1978**).
[7] Helliwell, R.A, *Radio Sci*., 18, 801, (**1983**).

[8] Inan, U.S., Bell, T.F. and Chang, W.H. *J. Geophys. Res*., 87, 6243, (**1982**).
[9] Vomcoridis J.L., Crystal, T.L. and Penavil, J, *J. Geophys Res*., 87, 1473, (**1990**).
[10]Carlson, C.R. and Helliwell, R.A. *J. Geophys Res*., 95, 15037, (**1990**).
[11] Moving, K.G. Godehard, H., Ronald, M. and Myczkowski, J. *J. Geophys. Res.*, 93**,** 5665-5683, (**1988**).
[12] Vomvoridis J.L.and Denavit, J. *Fluids*, 23, 174. (**1980**).
[13] Serra F.M.,"Nonlinear shift of wave parameters" *Planet Space -Sci*, 32, 985,(**1984**).
[14] Dungey J.W.,"Loss of vanallen electrons due to whistlers" *Planet Space Sci*, 11, 591, (**1963**).
[15] Starodubtsev M. and Kraft, C, *Physics of Plasmas* 6, 2598,(**1999**).
[1 6] Misra, K.D. and Haile, T, *J. Geophys Res*., 98, 9297, (**1993**).
[17] Huang, L., Hauikins, J.G. and Lee, L.C. *Journal of Geophys. Res*. 95, 3893, (**1990**).
[18] Misra K.D.and Pandey, R.S. *J. Geophys Res*., 100, 19405, (**1995**).
[19] Harris, E.G, Physics of hot plasma, Edited by R.Oliver and T.Boyd Edinburg, (**1970**).
[20]Pandey R. S., Pandey R. P., Karim, S.M., Srivastav A.K. and Hariom, *Progress in Electromagnetic Research* M 1,207- 217, (**2008**).
[21] R.S.Pandey and K.D.Misra, *Earth Planets Space*, 54, 159, (**2002**).